Silver Electrolysis for Disinfection of Spacecraft Potable Water: 2023 Update

Phillip M. Hicks[1], Rogelio Garcia Fernandez[1]
Jacobs Technology, Houston, TX, 77058, U.S.A.

and

Niklas Adam[2]
NASA Johnson Space Center, Houston, TX, 77058, U.S.A.

Anodic dissolution of silver electrodes, or "silver electrolysis," is being investigated as a means of introducing biocidal silver into potable water on exploration spacecraft. Last year's paper reported a fault condition termed "electrode bridging," in which silver deposits on interelectrode wetted materials, eventually bridging the electrode gap and providing an alternate conduction pathway that diminishes the silver output of the reactor. Since then, two strategies have been developed that prevent this fault from occurring: 1) increasing the frequency of polarity reversal and 2) separating the active surface of the electrode from the interelectrode wetted material. These strategies were tested independently, and in both cases, the reactor performed as expected with no occurrence of bridging for at least one crew-year equivalent of cumulative operation. Additional tests were conducted at varying levels of influent dissolved oxygen to better understand the nature of the cathode reaction and its impact on reactor performance. Results indicate that the primary cathode reaction is the reduction of dissolved oxygen, which could imply a dependence of reactor performance on dissolved oxygen concentration. However, it was found that at the typical oxygen concentrations anticipated for spacecraft processed water, the impact on silver electrolysis performance was negligible. Finally, multiphysics modelling of the reactor fluid mechanics and electrochemistry was undertaken to provide the capability to optimize the design of a future reactor prototype.

Nomenclature

A	=	cross-sectional area
Ag_k	=	silver concentration, calculated based on conductivity measurement (see Ref. 1)
C	=	mass-based concentration
DO	=	dissolved oxygen
DORB	=	dissolved oxygen removal bed
F	=	Faraday's constant
I	=	current
ICP-MS	=	inductively coupled plasma mass spectrometry
ISE	=	ion-selective electrode
IX	=	ion exchange
J	=	mass flux
κ, k	=	conductivity
φ	=	current efficiency
ppb	=	part per billion
µm	=	micro-meter, or micron
M_{Ag}	=	molar mass of silver
mA	=	milli-amp
µA/cm^2	=	micro-amp per centimeter squared
mg/L	=	milli-grams per liter solution
$\forall$	=	volumetric flowrate
z	=	charge number

[1] Project Engineer, Jacobs Technology – JETS II Contract, Jacobs Engineering (2224 Bay Area Blvd)
[2] Water Technology Engineer, Crew and Thermal Systems Division, Mail Stop: EC3 (2101 NASA Pkwy)

I. Introduction

Ionic silver at concentrations between 200-400 ppb is being considered as a replacement for iodine as the residual biocide in future spacecraft potable water systems. Specifically, a silver-ion-imparting technology is sought to replace the iodine-imparting resin in the product water segment of the water processor. Replacing iodine with silver requires an in-line method to accurately introduce the silver into water under conditions expected in a spacecraft water processor, which include low conductivity and low flowrate. Furthermore, the method should require little to no maintenance (including replacement of consumables) over the duration of a three-year mission. Finally, it must have reasonably low mass and volumetric footprint.

Silver electrolysis is a promising candidate technology for this purpose as it can be controlled and monitored via simple electrical parameters, it requires no moving parts, and it does not rely on a chemical resin that is depleted over time. Feasibility testing that was conducted last year demonstrated the capability of a silver electrolysis system to deliver a consistent silver concentration for a long duration and monitor the concentration via conductivity measurement.[1] This testing represented a major milestone in the development of the electrolytic silver dosing technology. However, it also uncovered a fault condition that occurs in some reactor configurations and modes of operation. The fault occurs when silver deposits on inter-electrode wetted surfaces and forms a conductive "bridge" between electrodes, resulting in diminished silver output. Early conclusions from that testing suggested the issue to be an engineering problem that could likely be resolved through optimization of reactor design, manufacturing, and system operation. Understanding and identifying strategies for preventing this phenomenon were major objectives of this past year, carried out under what is referred to in this paper as the "fault prevention test." Additionally, this paper also describes testing performed to better understand the role of dissolved oxygen in the cathode reaction and the preliminary results of an effort to develop a multiphysics model of the silver electrolysis reactor. These efforts are part of a continuing campaign to develop and design a flight-ready electrolytic silver biocide dosing system in support of NASA's future exploration goals.

II. Methods

A. Test Article

The silver electrolysis reactor proof-of-concept prototype (hereafter "reactor") that was used in feasibility testing[1] was also used for this test program. The reactor body consists of a polycarbonate base and lid that can be separated to allow the insertion of a variable number of parallel plate silver electrodes and interchangeable electrode-spacing components. The electrodes protrude through the reactor lid to enable electrical connection with quick-disconnect flag receptacles. The non-permanent nature of the water seal and electrical connection permit the electrodes to be removed for analysis and polishing. In combination with the interchangeable spacing components, this arrangement also permits the reactor to be placed in alternate configurations with varying numbers of electrodes and electrode spacing. For this test program, the design of the spacers was modified such that the discrete polypropylene inlet/middle/outlet spacers (both bottom and top) were replaced with slotted polycarbonate "floor" and "ceiling" spacers that spanned the entire reactor length. This modification ensured more accurate and consistent spacing of the electrodes and improved the top/bottom symmetry of the flow channels. For reactor configurations with less than the maximum number of electrodes, flow blockers were placed between the walls of the reactor cavity and the outermost electrodes to force all the flow between the electrodes. The modified reactor is shown in Figure 1.

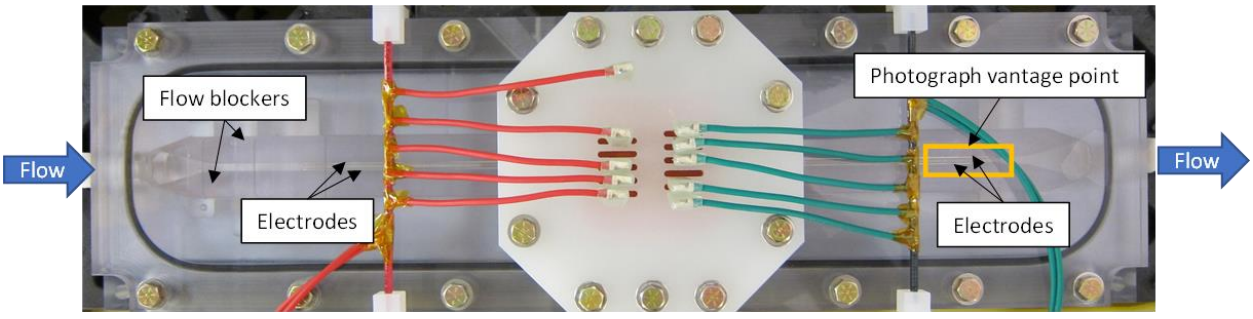

Figure 1. Silver Electrolysis Reactor Proof-of-Concept Prototype. *Reactor is depicted in the two-electrode configuration. The orange box is the approximate vantage point for the photographs in Figures 3, 5, and 7.*

B. Test Rig

The test rig used for this test program is depicted in Figure 2. The test rig is the same as that described in the paper on feasibility testing[1] with two minor modifications: 1) the inclusion of a second dissolved oxygen sensor upstream of the reactor, and 2) the addition of hardware that enabled control of the influent dissolved oxygen concentration. This hardware included a dissolved oxygen removal bed (DORB), an organic scavenger for removing contaminants released by the DORB, and two flowmeters with integrated metering valves that provided control over the amount of flow directed through the DORB. This dissolved oxygen removal hardware was only used in the dissolved oxygen portion of the testing: the items in the dashed box in Figure 2 were bypassed in the fault prevention test.

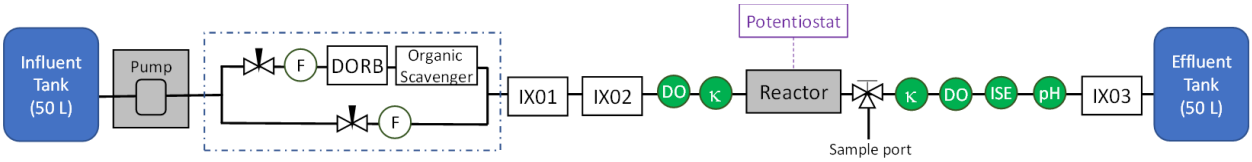

Figure 2. Functional Schematic of Test Rig

C. Test Execution (General)

Prior to each test case, the electrodes were hand-polished to a 1 µm finish, sonicated in a 1% solution of laboratory-grade detergent, wiped with an ethanol-soaked cotton ball, then rinsed thoroughly with deionized water. Inline sensors were calibrated weekly. Water samples were periodically retrieved from the sample port (Figure 2) during operation and analyzed for silver concentration using triplicate measurement of both inductively coupled plasma mass spectrometry (ICP-MS) and an offline ion selective electrode (ISE: Thermo Scientific 9616BNWP). Other aspects of test execution that were specific to either the fault prevention test or the dissolved oxygen test are reported in their respective sections.

III. Fault Prevention Test

A. Background

The electrode bridging fault, originally described in the paper on feasibility testing,[1] has now been consistently observed during reactor operation in which no preventive measures have been taken. In these instances, the fault resulted in diminished silver output and progressed to the point that the reactor was producing an insignificant silver concentration. This test program sought to characterize the phenomenon and determine mitigation strategies. To that end, multiple test cases were conducted in which a single parameter was varied to determine its impact on the electrode bridging fault.

B. Test Execution

The reactor was first tested in a baseline configuration from which the other test cases differed by only a single parameter. The baseline configuration included two electrodes (single cell) to minimize electrode preparation and any variability that may otherwise occur with multiple cells. The system was operated with a flowrate of 33 mL/min (a third of the expected water processor flowrate), such that the reactor emulated a single cell of a three-cell system. In practice, any reasonable number of cells could be combined in parallel, with additional cells reducing current density and applied voltage. The ultimate reactor design will likely have more electrode area than the three-cell system emulated, such that this test represented worst-case conditions and thus accelerated the identification of fault prevention strategies.

Similarly, polarity reversal was only used in the one test case that was specifically investigating the technique. It was omitted from all other test cases in order to test the effectiveness of other parameters under the worst-case condition of constant polarity. The intent is to combine the effective aspects of the successful test cases into a future reactor design whose reliability will be tested more thoroughly.

The reactor was operated at a current of 0.33 mA (current density of 3.8 µA/cm^2) for all but the polarity reversal case, as discussed below. This current was found to provide approximately 400 ppb of silver in the reactor effluent for the baseline configuration. A higher or lower silver concentration in each test case was thus indicative of improved or diminished current efficiency, respectively.

In all cases, the system was operated for up to eight hours per day and up to five days per week. Operation was continued until the reactor either failed or achieved a cumulative operation of 146 hours, which corresponds to one crew-year equivalent of operation.

C. Results

In several test cases, the altered parameter had limited impact on the electrode bridging phenomenon, and the reactor failed within the first eight hours of operation. These unsuccessful parameter changes included increased electrode gap (0.5 cm), altered surface of interelectrode material (rough rather than smooth), altered surface of electrode (600 grit rather than 1 μm), and aerated rather than ultrapure influent water. However, two conditions were identified that completely prevented the fault for at least one crew-year equivalent of operation with no indication of degrading performance. These test cases are described in subsections 2 and 3 after the baseline results are discussed in subsection 1.

1. Baseline Test Case

Because no fault prevention measures were employed in this test case, it provided a good representation of the electrode bridging fault. The fault was thus well-characterized by time-lapse photography taken of the electrode channel through the top of the reactor during operation (see Figure 3).

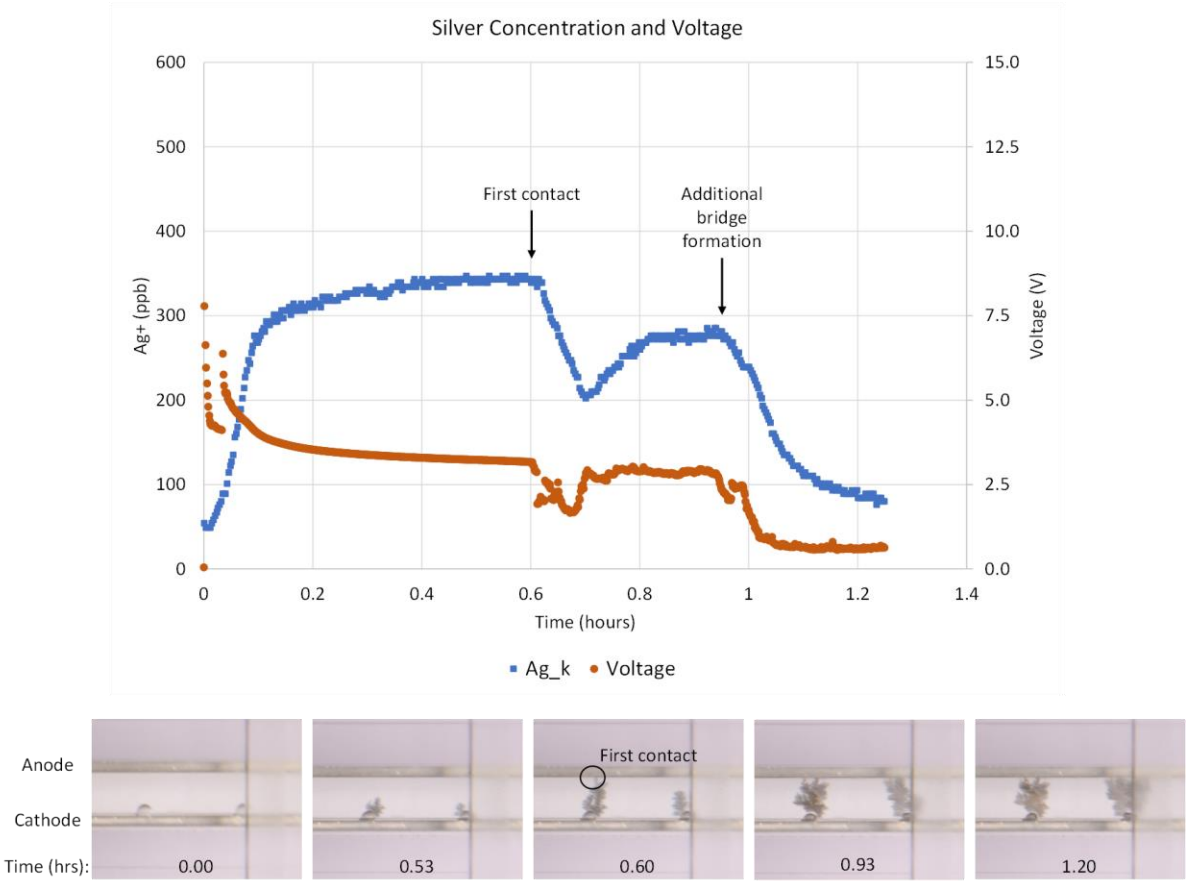

Figure 3. Electrode Bridging Fault: Data and Time-lapse. *The plot shows the silver concentration and voltage from an experiment conducted in the baseline configuration. The pictures are top-down photographs of the electrode channel (from the vantage point indicated in Figure 1) during the experiment at the indicated times. (The vertical line on the right side of each image is a feature on the reactor lid that affects the light transmission but not the physics since it is external to the electrochemical cell.) The scales of both y-axes were selected to be consistent with Figures 4 and 6 for the purpose of comparison.*

The time-lapse images confirm that the bridges are formed by silver deposits that nucleate at the cathode* and grow dendritically toward the anode, and that the voltage and silver concentration decline and/or become erratic once the first dendrite fully bridges the gap. In some cases, including that shown in Figure 3, the voltage and concentration exhibit a partial recovery until additional dendrites bridge the gap, at which point those parameters decline more decisively.

2. Polarity Reversal

In the feasibility testing discussed previously,[1] it was observed that periodically reversing the electrode polarity was very beneficial in prolonging reactor life, but it did not consistently prevent electrode bridging completely. In that test program, a thirty-minute polarity reversal half-cycle was employed (i.e. the polarity was reversed every thirty minutes). It was suspected that this half-cycle was long enough to permit substantial dendrite growth that could not be fully reversed on subsequent half-cycles, permitting the dendrites to ultimately bridge the electrode gap. Naturally, a shorter half-cycle was considered as a possible bridging prevention technique. However, because the silver concentration exhibits a transient dip with each reversal of polarity, an increase in reversal frequency is accompanied by a decrease in average silver output for a given current. Increasing the current (and thus silver concentration) comes at the cost of increased voltage, which tends to reduce current efficiency. Thus, the optimal reversal frequency is not obvious. For this test case, a 1-minute half-cycle was used with a current of 0.7 mA (current density of 8.2 µA/cm^2) since this current was found to output approximately 400 ppb silver. As shown in Figure 4, this frequency of polarity reversal enabled at least 146 cumulative hours (one crew-year) of operation with no indication of electrode bridging or other system degradation.

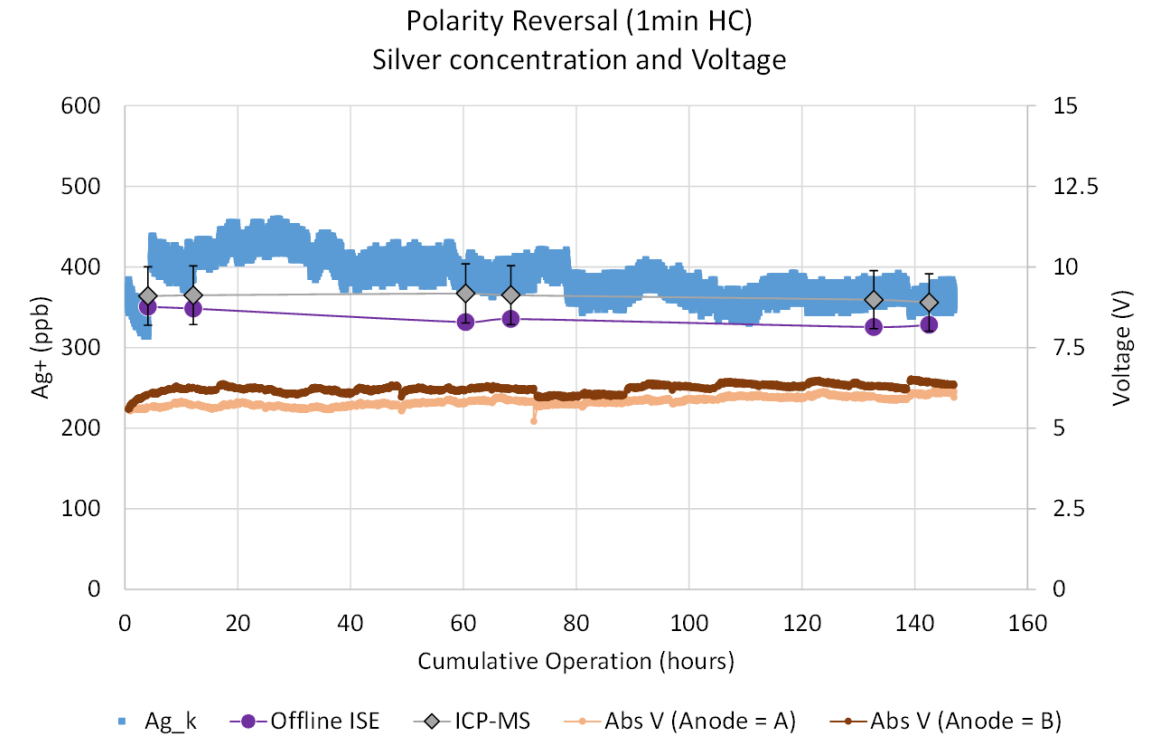

Figure 4. Polarity Reversal Data. *Silver concentration (Ag_k, Offline ISE, and ICP-MS) is plotted on the left axis, voltage on the right. The silver concentration measurements have an estimated instrument accuracy of ±10%; error bars are plotted only on the ICP-MS data to maintain readibility. The plotted voltage is the absolute value of the end-of-half-cycle voltage from each half-cycle. The voltage is plotted in two series to distinguish the "forward" and "reverse" half-cycles. Inline data (Ag_k and voltage) taken during sampling and system startup is omitted.*

* As seen in Figure 3, the dendrites nucleated at small air bubbles at the cathode/ceiling interface. It is worth noting that this was the only test case in which an obvious nucleation site was observed.

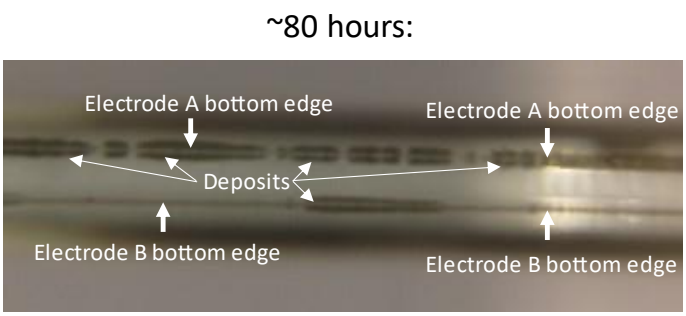

Figure 5. Deposits Observed During Polarity Reversal Test Case. *Top-down photograph of the electrode channel (from vantage point indicated in Figure 1) at approximately 80 hours of cumulative operation. Note that a mirror image of each deposit can be seen along the bottom edges of the electrodes.*

Although there was no electrode bridging, silver deposits were observed on the floor of the electrode channel along the bottom edges of the electrodes, as depicted in Figure 5. However, these deposits were distinct from those seen in all other test cases by two differences. First, they did not propogate across the electrode gap, but rather grew along the electrode edges. In fact, upon closer inspection after posttest reactor disassembly, it was noted that the deposits were almost completely amorphous, with very few dendritic features. Second, the deposits reached a steady-state about half-way into cumulative operation, after which there was no further growth (including growth along the electrode edge). The first silver deposit was observed about four hours into operation along the B electrode; after about eighty hours into operation, there were no observable changes in deposit size or shape. It was thus concluded that the increased polarity reversal frequency was successful in preventing the electrode bridging fault, though additional iterations of such testing would be required to demonstrate reliability.

3. Edge Masking

Notwithstanding the success of polarity reversal in preventing electrode bridging, complete prevention of silver deposits altogether would enhance current efficiency and also confidence in the reliability of the technology. To that end, another strategy was implemented in which electroplating tape was placed over the top and bottom edges of the electrodes. In this way, the portions of the electrodes in contact with the regions of lowest fluid velocity were masked from electrochemical reaction. This configuration separates the electrode surfaces from the electrode supports (interelectrode material) and decreases the propensity of silver ions to migrate across the electrode gap and cathodically reduce. (Incidentally, it also reduces the electroactive area, increasing the current density to 5.5 $\mu A/cm^2$ for this configuration.) It serves as a proof of concept for either masking the edges with a permanent coating or physically separating the electrodes from other wetted materials by minimizing and strategically locating the electrode supports. The benefits of this configuration were demonstrated by operating without polarity reversal; results are shown in Figure 6. Not only did the configuration prevent electrode bridging for at least one crew-year of operation, it also resulted in a significant increase in current efficiency over the baseline test case (~75% vs ~50%).

Thanks to the edge masking, no silver was deposited directly on the interelectrode materials. However, because polarity reversal was not employed, the silver ions that did electrochemically reduce gradually built up on the cathode, forming flakes that eventually broke off and settled on the reactor floor and/or washed downstream. Figure 7 provides photos exemplary of the initial formation (left image) and flake settling (right image). The first hint of flake formation was observed at thirty-six hours cumulative operation and the first settled flake was observed at ninety-six hours cumulative operation. Settled flakes would eventually disappear, likely having been carried downstream. This "cathodic flaking" is undesirable due to potential impacts on downstream systems and water potability; however, at this time it is not considered to be a significant concern given that it only occurred when polarity was not reversed. The combination of edge masking with polarity reversal is expected to provide long-lasting reactor operation with no silver deposits and no flakes. This expectation will be confirmed in future reliability testing.

4. Additional takeaways and conclusions

Even the test cases that were not successful in preventing electrode bridging provided useful insights. First, it was noted that silver deposits only formed in the downstream two-thirds (predominantly the final third) of the reactor. This is consistent with the cathodic deposition mechanism and the fact that the silver concentration increases in the direction of flow. Second, in test cases in which the reactor configuration included a sixteenth of an inch gap between the top edges of the electrodes and the reactor lid, silver did not deposit on the lid (the top of the electrode channel). This is in contrast to test cases in which the reactor configuration did not include this gap and silver consistently deposited on both the top and bottom of the electrode channel. These two observations indicate that electrode bridging only occurs in regions of high silver concentration in contact with interelectrode material. Finally, in a test case conducted with aerated deionized water (IX beds were bypassed and thus carbonate species not removed), the current

efficiency was significantly higher than in the baseline case (~90% vs ~50%), possibly due to 1) the higher conductivity of the water diminishing the migratory flux of the silver ions and 2) the lower pH of the water discouraging silver oxide formation. The time to failure from electrode bridging was only marginally improved in this test case, but the increased current efficiency is noteworthy. Taken together with the success of polarity reversal and edge masking in preventing the electrode bridging fault, these takeaways suggest several design and optimization strategies that are being considered for implementation in the next generation electrolysis reactor to improve the long-term stability and overall reliability.

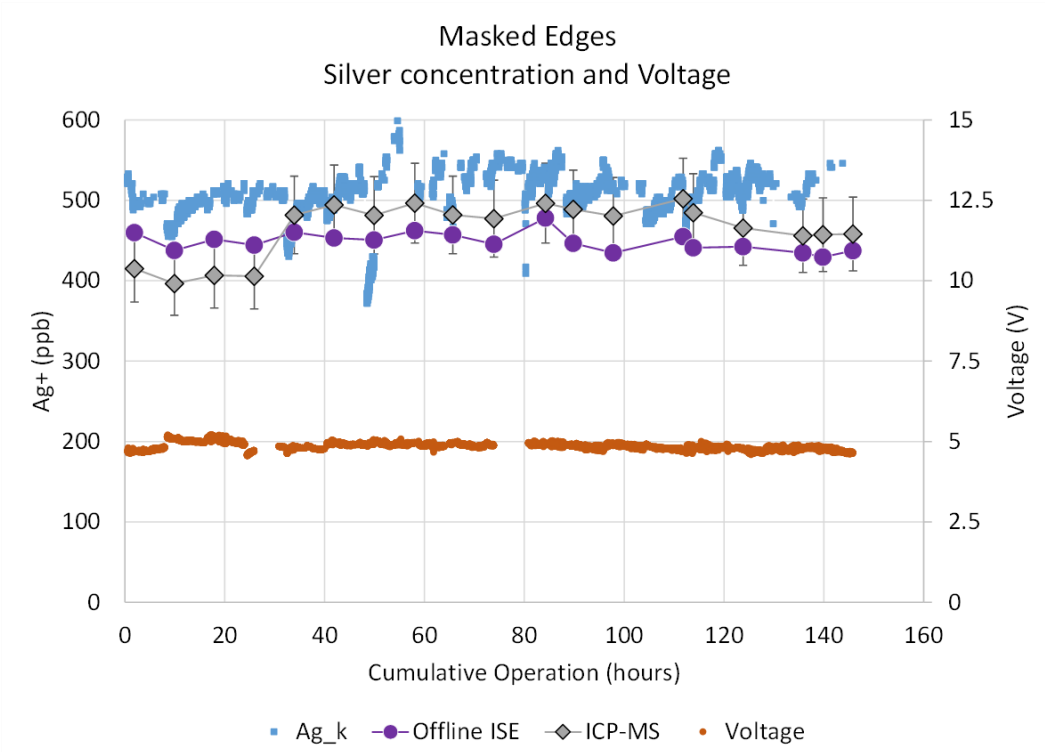

Figure 6. Masked-Edge Data. *Silver concentration (Ag_k, Offline ISE, and ICP-MS) is plotted on the left axis, voltage on the right. The silver concentration measurements have an estimated instrument accuracy of ±10%; error bars are plotted only on the ICP-MS data to maintain readibility. Inline data (Ag_k and voltage) taken during sampling and system startup is omitted. Voltage data is missing between hours 26–31 and 74–81 due to corruption of the data files, but the data was observed in real-time and was consistent with the rest of the voltage data.*

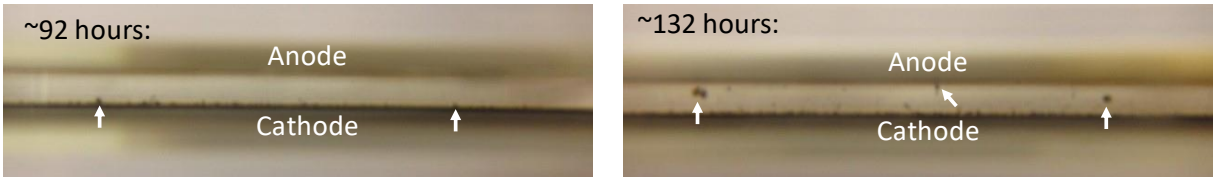

Figure 7. Cathodic Flakes Observed during the Masked-Edge Test Case. *Top-down photographs of the electrode channel from the vantage point indicated in Figure 1. The flakes are the dark specks (large ones indicated by arrows). In the photo on the right, the middle flake next to the anode actually formed at the cathode and later settled next to the anode, as pictured.*

IV. Dissolved Oxygen Test

A. Background

Although the anode reaction (silver dissolution) is the purpose of the reactor, the cathode reaction is an essential part of any electrochemical process and must be considered when investigating the overall performance of the system. Given the purity of the water processor product water, the only reducible species in the reactor electrolyte are dissolved oxygen, hydronium ions, and silver ions that have migrated from the anode. Thus, the primary cathode reaction is either reduction of dissolved oxygen (DO) or evolution of hydrogen, with a likely secondary reaction being the reduction of ionic silver. Oxygen reduction is the thermodynamically favored reaction, but kinetic limitations of this reaction may permit the hydrogen evolution reaction to proceed instead. Understanding the cathode reaction(s) is necessary for a solid grasp of the fundamentals of the reactor electrochemistry. In particular, it is important to determine if reactor performance is impacted by influent DO concentration. Prior to this test, all silver electrolysis testing had been performed with water in equilibrium with laboratory atmosphere (DO concentration of about 8.7 mg/L). The International Space Station water processor, which is the assumed baseline technology for future spacecraft water processing, may provide product water with a lower DO concentration. The DO concentration of the product water is not known empirically, but the minimum possible DO concentration can be calculated by assuming equilibrium between the water and the sweep gas in the water processor's gas separator. In this case, the DO concentration would be 5.5 mg/L; in reality, the DO concentration in the product water is probably higher. The purpose of this test was to investigate the cathode reaction and determine whether reactor performance is impacted by influent DO concentration.

B. Test Execution

The dissolved oxygen test consisted of two test cases at different currents. In TC01, the current was set to 0.75 mA (current density of 1.4 $\mu A/cm^2$) because it resulted in the target silver concentration of ~400 ppb. In TC02, the current was set to 3.0 mA (current density of 5.5 $\mu A/cm^2$), the maximum permissible current based on constraints of the test rig. The rationale for using the maximum current was to accentuate the DO consumption and make associated trends more apparent. Both test cases comprised multiple steps at varying influent DO concentration. Each step was a distinct experiment consisting of a stabilization period (to allow the DO concentration to reach its new steady-state value) followed by one hour of electrolysis at the test current. The DO concentration was controlled by varying the percentage of flow bypassing the dissolved oxygen removal bed (DORB) versus flowing through it. The flowrate was 100 mL/min. The reactor was placed in the ten-electrode configuration with a 0.25 cm electrode gap and electrode edges masked with electroplating tape. Electrode polarity was constant during each step but reversed between steps. In each step, the bias between the influent and effluent DO sensors was determined just prior to the initiation of electrolysis, and this bias was subtracted from the steady-state difference between the sensors to give the DO consumption. System performance was assessed by monitoring voltage, silver concentration, and DO consumption at the various influent DO concentrations.

C. Results

Figure 8 shows the steady-state voltage, silver concentration, and DO consumption from each step of the two test cases. An important observation is that the silver concentration was not impacted by influent DO concentration, and the voltage only started to increase when the DO concentration went below 2.5 mg/L. This voltage increase was probably the result of a combination of two factors: 1) an increase in mass transfer resistance (due to lower gradient between bulk and surface DO concentration) and 2) the onset of the hydrogen evolution reaction (as discussed below). Regardless, reactor performance was only impacted when the influent DO concentration was less than half the minimum expected concentration of 5.5 mg/L.

Another takeaway from the data is that dissolved oxygen reduction is the predominant cathode reaction when the influent DO concentration is above ~1 mg/L. This is determined by comparing the actual DO consumption with the theoretical value, where "theoretical" denotes the value that would be obtained if 100% of the cathodic current went toward the oxygen reduction reaction (indicated by dashed lines on the plot in Figure 8). One could think of the ratio of actual DO consumption to theoretical as the cathodic current efficiency for the oxygen reduction reaction. For influent DO concentration greater than 1 mg/L, oxygen reduction accounted for an average of 96% of the cathodic current in TC01 and 75% in TC02. The diminished oxygen reduction current efficiency in TC02 could be a result of increased cathodic silver reduction, which would also partially explain the significant drop in silver production current efficiency (second plot in Figure 8).

Below 1 mg/L influent DO concentration, it is apparent that another cathode reaction is occurring. This assertion is based on the sharp decline in oxygen consumption, the lack of significant change in silver concentration, the increase in voltage, and the fact that current is being held constant over each step of the two test cases. By process of elimination, it is assumed that the alternative reaction is the reduction of hydronium ion. While it is expected that this reaction will lead to the evolution of hydrogen in the reactor, such production is not considered to present a significant hazard. Even the most conservative hazard analysis performed to date, which assumed that hydrogen evolution accounts for 100% of the cathodic current, determined that the resultant rate of hydrogen production was low enough that the associated risk of hydrogen accumulation could be mitigated effectively with simple electronic controls. Nevertheless, future considerations of operational constraints and system optimization will be aided by better knowledge of the cathode reaction, such that additional investigation is warranted. At this point, we can conclude that when the influent DO concentration is in the range expected in spacecraft potable water, the predominant cathode reaction is reduction of dissolved oxygen and it does not impact reactor performance.

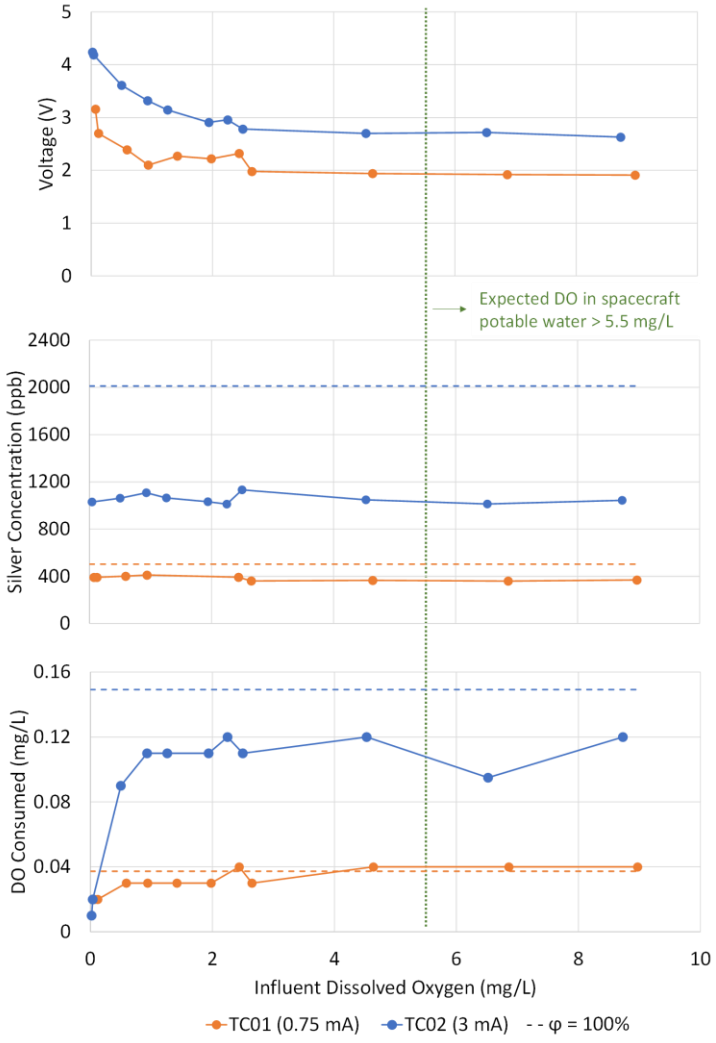

Figure 8. Dissolved Oxygen Test. *Horizontal dashed lines on the bottom two plots indicate the values that would be expected at 100% current efficiency (φ) of the reaction in question (silver production and oxygen consumption, respectively). For silver production, 100% efficiency also implies that no silver is cathodically reduced.*

V. Preliminary Modelling

A preliminary multiphysics model of the reactor has been developed using COMSOL Multiphysics® software.[2] This software provides user interfaces for coupled systems of partial differential equations and generates numerical solutions based on the finite element method. In our model, the fluid flow physics is coupled with the electrochemistry to model the electric potential and species concentrations. The electrochemistry study uses a tertiary current distribution, which combines the corresponding space-and-time-dependent transport partial differential equations with the appropriate electrode-based kinetics. This mathematical framework is appropriate for the modelling since the electrolyte composition in the reactor varies in space and time. The preliminary model is of a single rectangular electrode channel (or cell) with a subset of the electrode reactions modelled. So far, the incorporated reactions include the primary anode and cathode reactions and an anodic oxide formation reaction. In the instance of the model

discussed in this section, the input parameters (flowrate, current, cell geometry) match those of the baseline test case discussed in Section III.C.1.

Figure 9 shows the silver concentration in the electrode channel after fifteen minutes have elapsed from the initiation of electrolysis. This view shows the outlet as well as the top and anode side of the channel. As expected, the silver concentration increases in the direction of flow due to convection and the increase in local current density. Migration and diffusion of silver ions across the channel from the anode to the cathode result in the eventual buildup of silver at the cathode. The high silver concentration at the cathode illustrates why there is a propensity for cathodic silver deposition even though this reaction is not yet included in the model.

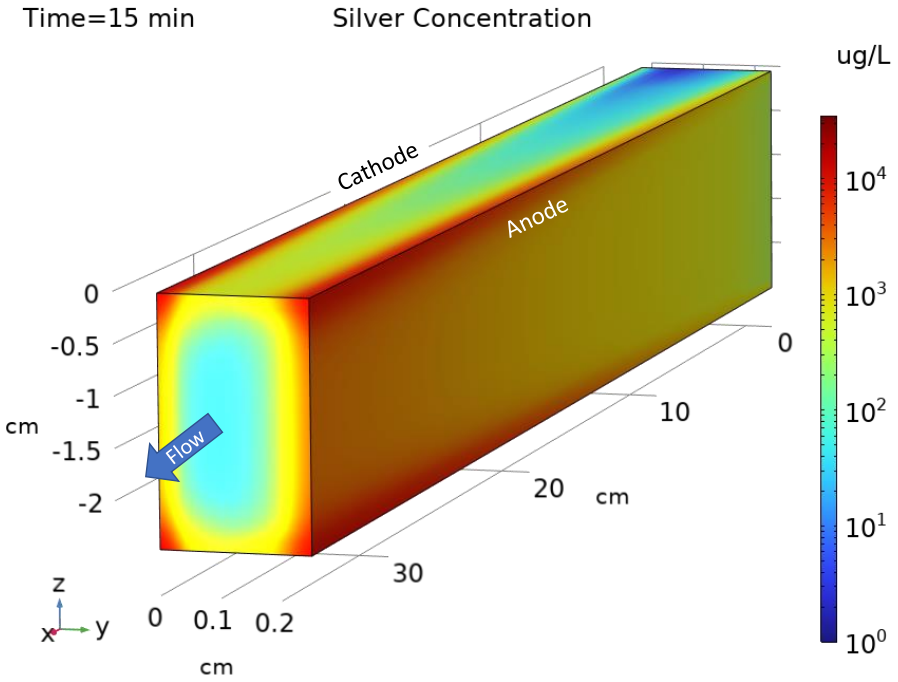

Figure 9. Preliminary Electrolysis Model. *Model of the silver concentration in the electrochemical cell at steady-state (fifteen minutes into the simulation). Note from the axes that the view is compressed in the x-direction and stretched in the y-direction for enhanced viewing of the silver concentration.*

A comparison of the model output with theoretical predictions and empirical data for silver concentration and voltage is shown in Figure 10. The ideal concentration, C_{ideal}, is the steady-state, mass-based silver concentration assuming 100% current efficiency. It is determined using the following version of Faraday's law, where M_{Ag} is the molar mass of silver, *z is* the charge number of the silver ion (equal to one), *F* is Faraday's constant, *I* is current, and $\forall$ is volumetric flowrate:

$$C_{ideal} = \frac{M_{Ag}}{zF} \cdot I/_{\forall} \tag{1}$$

C_{ideal} is the concentration that would be achieved in the absence of secondary reactions. It is represented in Figure 10 with a pink dashed line. The model concentration, C_{model}, is the average (over the outlet boundary) of the model-determined mass flux of silver ions, *J*, multiplied by the cross-sectional area of the outlet, *A*, divided by the volumetric flowrate, $\forall$:

$$C_{model} = \frac{J_{avg}A}{\forall} \tag{2}$$

It represents the fully-mixed silver concentration of the effluent of the electrode channel and is shown in Figure 10 with black lines (dotted and solid). Two iterations of the model were run: one with only the primary reactions included

(represented by the dotted line) and one with the primary reactions and an anodic oxide formation reaction. The fact that the steady-state value of the "primary reactions" version of the model output matches (approximately) the ideal value demonstrates that the model is appropriately balancing mass and charge. The incorporation of the anodic oxide secondary reaction (an inefficiency) makes the model more realistic and brings it into closer agreement with empirical data (both silver concentration and voltage). The discrepancy in transient silver concentration between the model and empirical data is expected: the empirical data was read by a sensor downstream of the reactor, such that the empirical data is delayed by the time it takes the fluid to reach the sensor and the slope of the curve is attenuated by mixing with the pure water that originally fills the space between the reactor and the sensor. The discrepancy in transient voltage behavior is not expected and is under investigation.

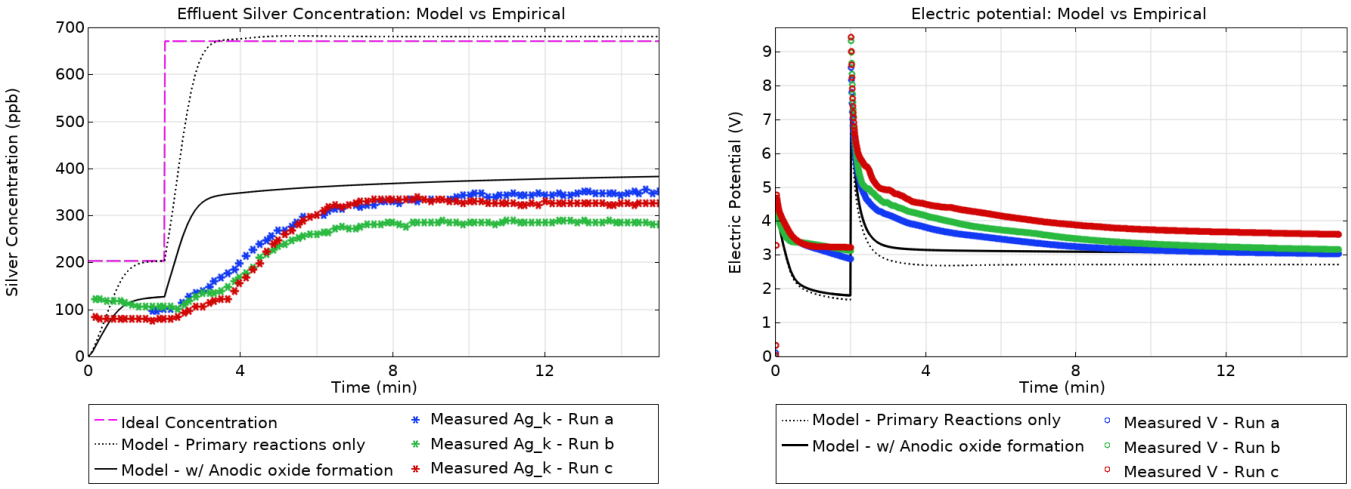

Figure 10. Comparison of Model, Theoretical, and Empirical Data. *In both the model and the test cases that generated the empirical data, the electrolysis was initiated at 0.1 mA for two minutes before being increased to the final current of 0.33 mA. This step up in current explains the steps up in both concentration and voltage at two minutes.*

Figure 11 shows the steady-state silver concentration at the outlet of the electrode channel (the outflow z-y plane in Figure 9) for both the baseline and masked-edge configurations. Comparing the two illustrates why the masked-edge configuration was effective in preventing the bridging fault and in raising the current efficiency. In the baseline configuration, the electrodes are active along their entire height, including in the corners of the electrode channel (where the electrodes contact the interelectrode material). The low fluid velocity in the corners enables accumulation of silver ions, and the low fluid velocity along the top and bottom of the channel enables silver ions to migrate to the cathode and dendrites to grow back toward the anode. By contrast, in the masked-edge configuration, the active surfaces of the electrodes are separated from the top and bottom of the channel, such that silver ions are not being released into the low-fluid-velocity regions, and any silver ions that are reduced on the cathode are not in contact with the interelectrode material.

The next step in the modelling process is to include other reactions that are known or suspected to occur in the reactor (such as cathodic silver deposition) and determine the appropriate kinetic parameters for each reaction. When this has been completed and the model has been validated against test data from multiple test configurations, it will be ready to serve as a predictive tool, including the ability to predict the current efficiency of various reactor designs. Furthermore, the ability of the model to determine silver concentration distribution will aid in identifying the optimal geometry for preventing electrode bridging. Having a virtual twin of this electrochemical system will enable model-based design optimization and accelerate the development of the next-generation reactor prototype.

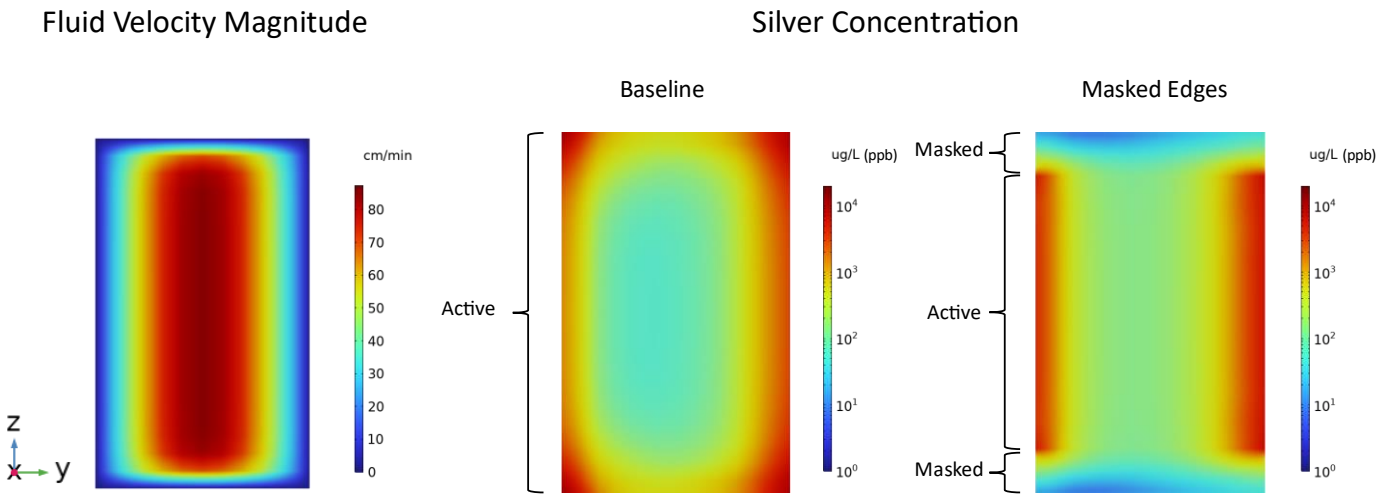

Figure 11. Steady-State Silver Concentration Distribution in Baseline and Masked-Edge Configurations. *The fluid velocity plot on the left applies to both silver concentration plots. The "Active" and "Masked" designations are shown on the cathode but apply to the anode as well.*

VI. Conclusions and Future Work

Silver electrolysis work in the past year consisted of fault prevention testing, dissolved oxygen testing, and multiphysics modelling. The fault prevention test demonstrated that the electrode bridging fault can be effectively prevented by either increased polarity reversal frequency or masking of electrode edges. The effect of edge masking could also be achieved by physical separation of electroactive surfaces from other surfaces, which could be implemented by careful design of electrode support geometry. A combination of approaches is expected to yield optimal performance. The dissolved oxygen test showed that dissolved oxygen consumption is the primary cathode reaction and that the influent dissolved oxygen concentration has negligible impact on reactor performance when it is in the range expected in water processor product water. Preliminary reactor modelling efforts have succeeded in establishing the theoretical soundness of the base model and the ability of the model to match empirical results by including secondary reactions. Efforts are underway to increase model complexity and realism with the ultimate goal of using the model to aid in reactor design optimization. The knowledge gained from each of these efforts is being applied to the design of a next-generation prototype that will be used to characterize the effectiveness and reliability of the technology for long-duration space missions.

Acknowledgments

The authors would like to thank the Exploration Capabilities, Life Support Systems Project for their support of this research as well as the countless colleagues who provided advice, sample analysis, assistance with reactor design and test rig development, and editorial suggestions. Special thanks to Moses Navarro for his suggestion to mask the electrode edges, Andrew Lin for his development of the oxygen removal system, and Zac Colovos for establishing the setup of the time-lapse photography.

References

[1] P. Hicks and N. Adam, "Feasibility Testing of Silver Electrolysis for Disinfection of Spacecraft Potable Water Systems," in *International Conference on Environmental Systems*, St. Paul, 2022.
[2] COMSOL Multiphysics® v. 6.1. www.comsol.com. COMSOL AB, Stockholm, Sweden.